Enhanced focus steering abilities of multi-element therapeutic arrays operating in nonlinear regimes

P. Yuldashev, S. Ilyin, L. Gavrilov, O. Sapozhnikov, W. Kreider, and V. Khokhlova

Citation: AIP Conference Proceedings **1685**, 040005 (2015); doi: 10.1063/1.4934400
View online: http://dx.doi.org/10.1063/1.4934400
View Table of Contents: http://scitation.aip.org/content/aip/proceeding/aipcp/1685?ver=pdfcov
Published by the AIP Publishing

Enhanced Focus Steering Abilities of Multi-element Therapeutic Arrays Operating in Nonlinear Regimes

P. Yuldashev[1,a)], S. Ilyin[1], L. Gavrilov[2], O. Sapozhnikov[1,3], W. Kreider[3] and V. Khokhlova[1,3]

[1]*Physics Faculty, Moscow State University, Leninskie Gory, 119991 Moscow, Russian Federation*
[2]*Andreyev Acoustics Institute, 4 Schvernik Str., 117036 Moscow, Russian Federation*
[3]*Center for Industrial and Medical Ultrasound, Applied Physics Laboratory, University of Washington, 1013 NE 40th, Street, Seattle, WA 98105, USA.*

[a)]Corresponding author: petr@acs366.phys.msu.ru

Abstract. Steering abilities of a typical HIFU therapeutic array operated in linear and nonlinear regimes were compared using numerical simulation with the 3D Westervelt equation. The array included 256 elements of 1.2 MHz frequency and 6.6 mm diameter distributed in a quasi-random pattern over a spherical shell with a 130 mm aperture and a focal length of 120 mm. In the case of linear focusing, thermal effects are proportional to the intensity level and the criterion for safe array operation is that the intensity in the grating lobes should be less than 10% of the intensity in the main focus. In the case of nonlinear focusing, the heating effect is no longer proportional to intensity; therefore the heat deposition rate was chosen as the relevant metric, using the same 10% threshold for the secondary lobe in comparison with the focal maximum. When steering the focus, the same linearly predicted intensity level at the main focus was maintained by increasing the array power. Numerical simulations of the acoustic field were performed for nonlinear propagation both in water and in tissue. It was shown that for shock-forming conditions in the main focus, the steering range of safe electronic focusing is larger than that for linear propagation conditions. Nonlinear sonication regimes therefore can be used to enlarge tissue volumes that can be sonicated using electronic steering of the focus of HIFU arrays.

INTRODUCTION

Multi-element phased arrays are used in many modern high intensity focused ultrasound (HIFU) surgical systems [1]. Such arrays enable complex beamforming to avoid overheating of obstacles, for example ribs, and phase and amplitude corrections to improve focusing through inhomogeneities in soft tissues and through skull bones [2, 3]. Electronic steering of the focus is also used to sonicate tissue volumes without mechanical movement of the transducer [4].

The steering range is a key metric for arrays with regard to their safety and efficacy in surgical applications. Enlarging the safe steering volume in tissue is important clinically; in particular, the importance of this problem has been widely discussed for HIFU applications in brain [3]. Steering of the focus can be performed only within certain limits, which are determined by two main factors. The first factor is related to generation of secondary grating lobes, which can result in unintentional damage of intervening tissues. Formation of grating lobes strictly depends on the positioning scheme of the elements. For example, regular positioning results in very strong grating lobes preventing large displacements of the focus [5]. Arrays with a quasi-random distribution of elements have much smaller grating lobes, and were shown to provide focus steering up to 10-15 mm [4, 5]. The second factor is the decrease of intensity in the steered focus due to the directivity pattern of each array element. Smaller elements are less directional and thus provide better steering abilities in an array. A directivity-related decrease in the intensity of the steered focus can be compensated by a corresponding increase of intensity at the elements to generate the same intensity as in the non-steered focus. However, power output of the elements has its own technical limits (imposed by heating, for example), which correspondingly restrict possible intensity compensation.

Recent Developments in Nonlinear Acoustics
AIP Conf. Proc. 1685, 040005-1–040005-4; doi: 10.1063/1.4934400

Nonlinear propagation effects have been shown to provide various advantages for HIFU applications. For example, tissue is heated much more effectively when shock fronts are formed at the focus [6]. The heat deposition rate for waveforms with a shock front can be about one order greater than that for a linear wave of the same pressure amplitude. Since shock formation in the focal region of the beam requires intensities that exceed a certain amplitude threshold, this effect can be used to diminish thermal effects in grating lobes where the intensity remains below the threshold [7]. The goal of this work was to compare steering abilities of a typical array operated in linear and nonlinear regimes [8]. The acoustic field of the array was simulated using a nonlinear propagation model based on the 3D Westervelt equation [9]; peak pressure, intensity, and heat deposition power in both the focus and the grating lobes were compared for linear and nonlinear propagation conditions.

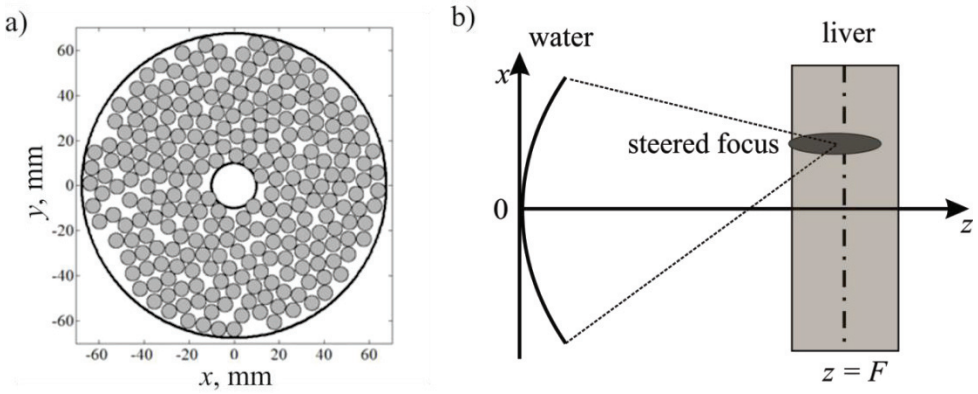

FIGURE 1. (a) Distribution of radiating elements at the surface of a therapeutic array; (b) geometry of the numerical experiment: array focus is electronically steered within 5 cm thick tissue layer (liver) centered around the geometric focus of the spherical shell ($z = F$).

NUMERICAL MODEL

In this work a multi-element therapeutic array which is a part of clinical HIFU therapy system (Sonalleve V1, 3.0T, Philips Healthcare) was chosen to investigate focus steering under strongly nonlinear propagation conditions [8]. The transducer included 256 elements of 1.2 MHz frequency and 6.6 mm diameter distributed in a quasi-random pattern over a spherical shell with a 130 mm aperture and a focal length of 120 mm. A front view of element positions in the plane (x,y) is shown in Fig. 1a. The configuration of the numerical experiment is sketched in Fig.1b. Here the array focus is steered laterally in a 5 cm thick layer of tissue (liver), with the non-steered focus position ($z = F$) in the center of steered target locations. The space between the array and tissue layer is filled by water.

A 3-D Westervelt equation was used to simulate the nonlinear acoustic field generated by the therapeutic array:

$$\frac{\partial^2 p}{\partial \tau \partial z} = \frac{c_0}{2}\Delta p + \frac{\beta}{2\rho_0 c_0^3}\frac{\partial^2 p^2}{\partial \tau^2} + \frac{\delta}{2c_0^3}\frac{\partial^3 p}{\partial \tau^3} + L(p). \quad (1)$$

Here $\tau = t - z/c_0$ is the retarded time, $\Delta p = \partial^2 p/\partial z^2 + \partial^2 p/\partial x^2 + \partial^2 p/\partial y^2$, parameters c_0, β, ρ_0 and δ are the ambient sound speed, nonlinearity coefficient, density of the medium, and the diffusivity of sound, respectively. Equation (1) accounts for the combined effects of nonlinearity, diffraction, thermoviscous absorption and power-law absorption in tissue, which is represented by the $L(p)$ term.

The boundary condition for the Westervelt equation was set at the plane (x, y, $z = 0$) at the apex of the spherical shell of the array. This was accomplished in two steps. First, the Rayleigh integral was used to calculate acoustic pressure at the plane (x, y, $z = 40$ mm):

$$p(\vec{r},t) = -i\rho_0 f \int_S \frac{u(\vec{r}')\exp(ik|\vec{r}-\vec{r}'|)}{|\vec{r}-\vec{r}'|}dS'. \quad (2)$$

Here $\vec{r} = \{x, y, z\}$, $u(\vec{r}')$ is the complex amplitude of the vibration velocity on the surface S' of the radiating elements, and $k = \omega/c_0$ is the wave number. Then the angular spectrum method was used to linearly back propagate the pressure distribution from the plane (x, y, $z = 40$ mm) to the plane (x, y, $z = 0$). The numerical algorithm is

described in detail in earlier publications [8, 9]. The intensity of the acoustic field radiated by each element of the array was set to 5 W/cm^2, which is sufficient to generate high amplitude waveforms with shocks at the focus [8]. The array focus was moved in the transverse direction from the center of curvature (0,0,120 mm) to the position (F_x,0,120 mm), where F_x is the focus shift by applying different phase delays to each element in the initial Rayleigh integral calculations.

Parameters of the numerical scheme were set as follows: longitudinal step $dz = 0.075$ mm, transverse steps $dx = dy = 0.025$ mm. The maximum number of harmonics retained in calculations was limited to 800. The values of the physical constants in Eq. (1) were chosen to represent typical conditions in water and liver at room temperature (20° C): $\rho_0 = 998$ kg/m^3, $c_0 = 1485$ m/s, $\beta = 3.5$, $\delta = 4.33 \cdot 10^{-6}$ m^2/s for water and $\rho_0 = 1050$ kg/m^3, $c_0 = 1580$ m/s, $\beta = 4.0$, $\delta = 4.33 \cdot 10^{-6}$ m^2/s for liver. The coefficient in the power law absorption in liver was 8.4 m^{-1} at 1.2 MHz and linear growth of the absorption with frequency was assumed.

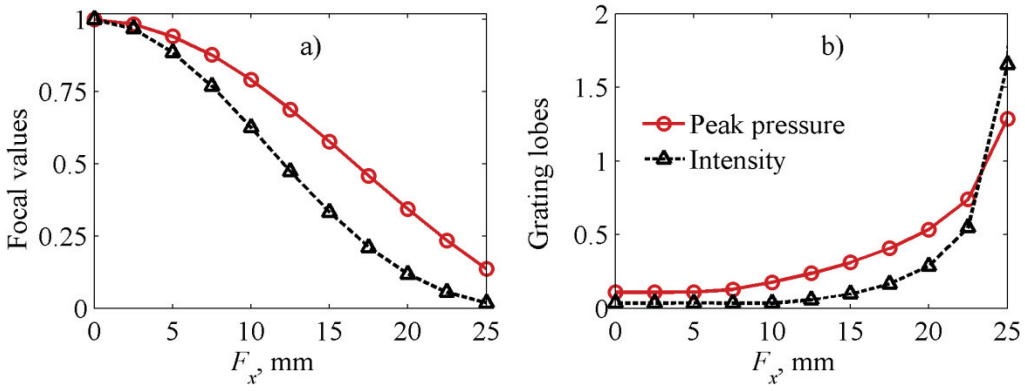

FIGURE 2. (a) Focal peak pressure (solid line) and intensity (dashed line) when the focus is steered to the position (F_x, 0, 120 mm), with values normalized relative to those at the non-steered focus; (b) increase of the peak pressure and intensity in grating lobes relative to the peak pressure and intensity in the steered focus.

RESULTS

Array steering capabilities in the case of linear propagation are summarized in Fig. 2. Decrease of the focal peak pressure (solid line) and intensity (dashed line) relative to peak pressure and intensity in non-steered focus is shown in the Fig. 2a and increase of the peak pressure and intensity in grating lobes relative to peak pressure and intensity in the steered focus is shown in the Fig. 2b. It is seen that focal pressure relative to the non-steered focal maximum decreases to 0.7 (-3 dB) at 12 mm steering and to 0.5 (-6 dB) at 17 mm. Thus, to steer the focus at 12 mm the array must be capable to increase power by a factor of 2 and to steer at 17 mm by a factor of 4 to compensate focal intensity decrease. In the case of linear focusing, thermal effects are proportional to the intensity levels. It is commonly accepted that the criterion for safe array operation is that the intensity in the grating lobes should be less than 10% of the intensity in the main focus. In our case this criterion is met for focus displacements up to 15 mm (Fig.2b). At greater focus displacements the intensity in grating lobes grows rapidly and at 23 mm it becomes equal to the intensity in the steered focus.

Nonlinear propagation effects resulted in a strongly distorted focal waveform with 70 MPa peak positive pressure and shock-front amplitude of 50 MPa. In the modeling, it was verified that parameters of nonlinear waveforms remained almost the same when the focus was steered and array power was compensated to maintain the same amplitudes in steered and non-steered foci. Peak positive pressure, intensity, and heat sources in grating lobes relative to the corresponding values in the steered focus are compared in Fig. 3 for linear and nonlinear propagation regimes. It is seen that in the nonlinear regime the peak positive pressure in grating lobes is much smaller in comparison to the linear propagation case (Fig. 3a). This result is caused by nonlinear amplification of the peak positive pressure at the focus of nonlinear ultrasound beams [9]. The intensity in grating lobes does not change too much between nonlinear and linear regimes (Fig. 3b). Note, that when nonlinear propagation effects are taken into account, the heating effect is no longer proportional to intensity. Also, when the shock front is formed, the heat deposition rate is about one order of magnitude higher than in the case of a linear wave with the same amplitude [6].

Accordingly, significant differences are predicted for heating in grating lobes in linear and nonlinear regimes relative to those in the main foci (Fig. 3c). At 15 mm steering linear heat sources in grating lobes are about 10 % of the focal values (similar to intensity) while nonlinear heat sources are still very low (about 2%). At 17.5 mm steering heat sources in the nonlinear regime remain the same (2 %); however, in the linear regime heat sources are higher than 15 %.

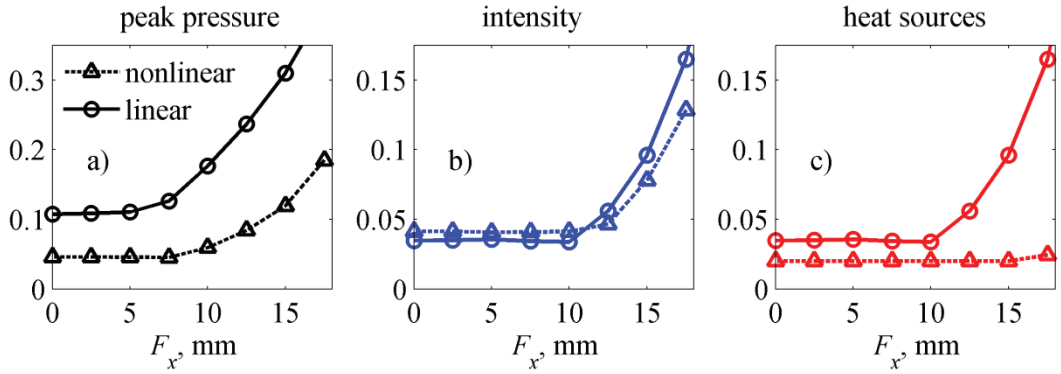

FIGURE 3. (a) Increase of the peak pressure in grating lobes relative to the peak pressure in the steered focus in linear (solid line, circle markers) and nonlinear (dashed line, triangle markers) propagation cases; (b) same for intensity; (c) same for heat sources.

CONCLUSIONS

In this work, the steering abilities of a typical therapeutic array were investigated in linear and nonlinear regimes using numerical simulations with the 3D Westervelt equation. It was shown that for shock forming conditions in the main focus, the steering range of safe electronic focusing is larger than that for linear propagation conditions. Nonlinear regimes therefore can be used to enlarge tissue volumes that can be sonicated using electronic steering of the focus of HIFU arrays.

ACKNOWLEDGMENTS

Work supported by RFBR 14-02-31878 and NIH NIBIB EB007643.

REFERENCES

1. M. Pernot, J.-F. Aubry, M. Tanter, J.-L. Thomas and M. Fink, Phys. Med. Biol.**48** (16), 2577 – 2589 (2003).
2. K. Hynynen, N. McDannold, G. Clement, F.A. Jolesz, E. Zadicario, R. Killiany, T. Moore and D. Rosen, European Journal of Radiology **59** (2), 149 – 156 (2006).
3. B. Quesson , M. Merle, M. O. Köhler, C. Mougenot, S. Roujol, B.D. De Senneville and C. T. Moonen, Med. Phys. **37** (6), 2533 – 2540 (2010).
4. J. W. Hand, A. Shaw, N. Sadhoo, S. Rajagopal, R. J. Dickinson and L. R. Gavrilov, Phys. Med. Biol., **54** (19), 5675 – 5693 (2009).
5. L. R. Gavrilov and J. W. Hand, IEEE Trans. Ultrason. Ferroelec. Freq. Contr. **41** (1), 125 – 139 (2000).
6. E. A. Filonenko and V. A. Khokhlova, Acoust. Phys. **47** (4), 468 – 475 (2001).
7. P. V. Yuldashev, S. M. Shmeleva, S. A. Ilyin, O. A. Sapozhnikov, L. R. Gavrilov and V. A. Khokhlova, Phys. Med. Biol. **58**, 2537 – 2559 (2013).
8. W. Kreider, P. V. Yuldashev, O. A. Sapozhnikov, N. Farr, A. Partanen, M. R. Bailey and V. A. Khokhlova, IEEE UFFC, **60** (8), 1683 – 1698 (2013).
9. P. V. Yuldashev, V. A. Khokhlova, Acoust. Phys. **57** (3), 334 – 343 (2011).
10. O. V. Bessonova, V. A. Khokhlova, M. R. Bailey, M. S. Canney and L. A. Crum, Acoust. Phys. **55** (4), 463 – 473 (2009).